

Transition from Van Vleck Paramagnetism to Induced Antiferromagnetism in $Tb_{\zeta}Y_{1-\zeta}Sb$

BERNARD R. COOPER

General Electric Research and Development Center, Schenectady, New York 12301

AND

OSCAR VOGT

Laboratorium für Festkörperphysik, ETH, Zürich, Switzerland

(Received 19 September 1969)

Low-field susceptibility and high-pulsed-field magnetization experiments have been performed on single crystals of $Tb_{\zeta}Y_{1-\zeta}Sb$ across the entire composition range from YSb to $TbSb$. As the terbium concentration increases, the magnetic behavior shows a transition from Van Vleck paramagnetism to antiferromagnetism at low temperatures at a Tb concentration of 40.3%. We attribute this antiferromagnetic ordering to an induced-moment effect in the Γ_1 singlet crystal-field ground state pertinent to Tb^{3+} in an octahedral crystal field. The crystal-field strength remains essentially constant, while the average exchange field varies approximately linearly with changing terbium concentration. We show that the behavior for small magnetic fields in the paramagnetic regime ($\zeta \leq 0.403$) and at or near the Néel temperature in the antiferromagnetic regime ($\zeta \geq 0.403$) can be understood on the basis of a linear molecular-field theory involving one crystal field and one exchange parameter. Analysis of the small-moment data gives an energy splitting, in the absence of exchange, of 11.9°K from the Γ_1 crystal-field singlet ground state to the Γ_4 triplet first excited state of the Tb^{3+} ion. We show that high-field anisotropic magnetization measurements at 1.5°K in the paramagnetic regime ($\zeta \leq 0.403$) indicate a significant contribution at large magnetization from higher-order anisotropic effective exchange; and we discuss how such measurements can be used to study the orbital contribution to effective exchange interaction.

1. INTRODUCTION

FOR rare-earth compounds, it is possible for the crystal-field effects to be comparable to, or dominant over, the exchange effects. Such a situation can lead to a number of interesting magnetic properties. The most striking situation occurs when the crystal-field-only ground state of the rare-earth ion is a singlet. Then as exchange increases, magnetic ordering at zero temperature occurs not through the usual process of alignment of permanent moments, but rather through a polarization instability of the crystal-field-only singlet ground-state wave function.¹

For such materials, theory²⁻⁵ predicts the existence of a threshold value for the ratio of exchange to crystal-field interaction necessary for magnetic ordering even at zero temperature. The present paper has two major features. First, we present the results for and discuss low-field susceptibility and high pulsed field magnetization experiments on mixed terbium-yttrium antimonide (NaCl structure) which directly exhibit the threshold exchange effect for induced magnetic ordering. This is done by showing the transition from Van Vleck paramagnetism to antiferromagnetism at low temperature as the fraction of terbium increases. Second, we discuss how high-field anisotropic magnetization

measurements⁶ in the paramagnetic regime can be used to provide basic information on the orbital effects on effective exchange interaction.

Both Tm^{3+} and Tb^{3+} have $J=6$ in their ground-state multiplets. Thus the same crystal-field Hamiltonian and crystal-field energy-level scheme used for Tm^{3+} in the preceding paper⁷ (referred to as I hereafter) apply to Tb^{3+} in the NaCl structure. [See Eqs. (2.1) and (2.11), and Fig. 1 of I.] As discussed in I, there is considerable evidence that the crystal-field effects for the Tm-group-V compounds of NaCl structure are predominantly fourth order [$x \approx -1$, $B_6 \approx 0$ in (2.1) or (2.11) of I]. We assume in the discussion of this paper that the same holds true for the corresponding Tb compounds, in particular $TbSb$. (Actually, the magnetization has little change from the fourth-order-only behavior until the sixth-order anisotropy is quite substantial, say $x > -0.6$. So this is not a very strong assumption. Furthermore, in Sec. 3 B we show that sixth-order anisotropy effects would not explain anomalous high-field magnetization behavior which we associate with orbital effects on the exchange.) Then the crystal-field level scheme for Tb^{3+} in $TbSb$ is given by Fig. 1 of I, and we reproduce this figure as Fig. 1 of the present paper.

The Γ_1 singlet ground state means that there is no permanent moment associated with either a Tm^{3+} or a Tb^{3+} ion in the octahedral crystal field. However, an applied magnetic field mixes some Γ_4 state into the Γ_1 state, and [see Eq. (2.10) of I] this polarization

¹ For a review of this effect see B. R. Cooper, *J. Appl. Phys.* **40**, 1344 (1969). The present results are referred to and briefly discussed in that review.

² G. T. Trammell, *J. Appl. Phys.* **31**, 362S (1960); *Phys. Rev.* **131**, 932 (1963).

³ B. Bleaney, *Proc. Roy. Soc. (London)* **A276**, 19 (1963).

⁴ B. R. Cooper, *Phys. Rev.* **163**, 444 (1967).

⁵ Y. L. Wang and B. R. Cooper, *Phys. Rev.* **172**, 539 (1968); *Phys. Rev.* **185**, 696 (1969).

⁶ O. Vogt and B. R. Cooper, *J. Appl. Phys.* **39**, 1202 (1968).

⁷ B. R. Cooper and O. Vogt, preceding paper, *Phys. Rev.* **B 1**, 1211 (1970) (referred to as I throughout the present paper).

process gives rise to the Van Vleck temperature independent susceptibility at low temperature. In a similar way a molecular field can induce a moment in the Γ_1 state. However, in the absence of applied field, the existence of a molecular field presupposes the existence of an ordered moment. This leads to a threshold condition on the exchange for magnetic ordering by such a process.

Now TbSb orders antiferromagnetically with $T_N \approx 15.1$ °K, while TmSb does not order magnetically at all. In fact, such a comparison holds for all of the Tb and Tm-group-V compounds of NaCl structure.⁸ The Tb compounds order, and the Tm compounds do not. Qualitatively this is quite reasonable in the induced magnetization picture. Both Tm^{3+} and Tb^{3+} have $J=6$; however, for Tb^{3+} $L=3$ and $S=3$; while for Tm^{3+} , $L=5$ and $S=1$. Since one expects the strength of the exchange to increase with S , and the strength of the crystal field to increase with increasing L , one expects the ratio of exchange interaction to crystal-field energy to be decidedly larger for Tb^{3+} than for Tm^{3+} . Then the fact that the Tb compounds order, and the Tm compounds do not, can be understood by the ratio of exchange to crystal-field energy exceeding the ordering threshold for Tb, and being below threshold for Tm.

The motivation for studying the magnetic behavior of the $\text{Tb}_x\text{Y}_{1-x}\text{Sb}$ system as terbium concentration varies is then quite simple. Yttrium is essentially identical to the heavy rare earths in its valence electron behavior, but has an empty $4f$ shell. Thus substituting Y for Tb essentially does not change the crystal field, but does reduce the effective exchange field acting on a given Tb^{3+} ion. In this way one can hope to reduce the exchange below the critical value necessary for magnetic ordering. As discussed below, we find that this picture is quite well justified, and experimentally the transition from Van Vleck paramagnetism to antiferromagnetism occurs as the Tb concentration increases above 40.3%.

For Tb concentrations below threshold, analysis of the upward shift of the inverse susceptibility with increasing Tb concentration allows determination of the exchange parameter giving the effective exchange field when that effective field varies linearly with the magnetization. The analysis also yields the value of W , the parameter giving the crystal-field splittings. Quite good agreement is found between the experimental behavior of $1/\chi$ versus T as ζ increases toward the ordering threshold value and the theoretical behavior expected for a molecular field varying linearly with the magnetization. For ζ above the threshold value for antiferromagnetic ordering, correspondingly good agreement is obtained for the values of T_N . However, for the high-field anisotropic magnetization in the paramagnetic regime, there is significant departure from the linear molecular field theory behavior. This is expected

⁸ G. Busch, J. Appl. Phys. **38**, 1386 (1967).

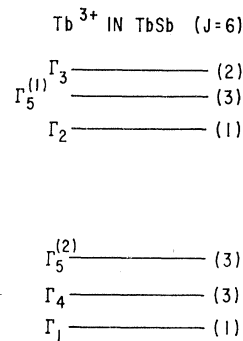


FIG. 1. Crystal-field level scheme for Tb^{3+} in a site of octahedral symmetry. Order of levels shown is for predominantly fourth-order anisotropy.

to be the case in systems such as this, where there are large orbital contributions to the magnetic moment. We then discuss how such high-field anisotropic magnetization experiments may be valuable in providing basic information on the orbital effects on effective exchange interaction.

2. EXPERIMENTAL PROCEDURE AND RESULTS

Mixed crystals of $\text{Tb}_x\text{Y}_{1-x}\text{Sb}$ have been made across the entire composition range. The samples are prepared by reacting appropriate amounts of Tb and Y turnings (not thicker than 2/100 mm) with chunks of Sb in closed evacuated silica tubes. All the metals used were of the highest commercially available purity. The primary reaction is complete after about 10 days at 600°C. The resulting powder (90% of which has the NaCl structure) is pressed into pellets of 8 mm diam and 6–8 mm length. These pellets are placed in a 40-mm-long tubular molybdenum crucible with an outside diameter of 14 mm and a 1-mm wall thickness. An insertion cap, which is 20 mm long with a ½-mm wall, is placed in the crucible leaving an open space of 20 mm. The cap is sealed under vacuum to the crucible by welding their top edges in an electron beam. The sealed crucibles are then placed in a vacuum graphite furnace with the crucible and heating element in a coaxial configuration. The heating element of the furnace is a double helix with 30-mm i.d. and 80-mm heating length. The bottom of the crucible, where the pellet is located, is in the center of the heating element, which is brought to approximately 2200°C. Under the influence of the temperature gradient between the bottom and the top of the crucible (the top of the crucible being the bottom of the insertion cap), the pellets evaporate and within about one week crystals are deposited at the top of the crucible (colder end).

The crystals have a cubic shape with a few mm cube length. They always cleave in $\{100\}$ planes, making shaping easy and permitting orientation by the Laue technique. The homogeneity of the samples was tested by a microprobe analysis. In the worst cases a concentration gradient of 2% along the whole crystal was observed. The Sb concentration remained constant while the intensities of Tb and Y decreased and in-

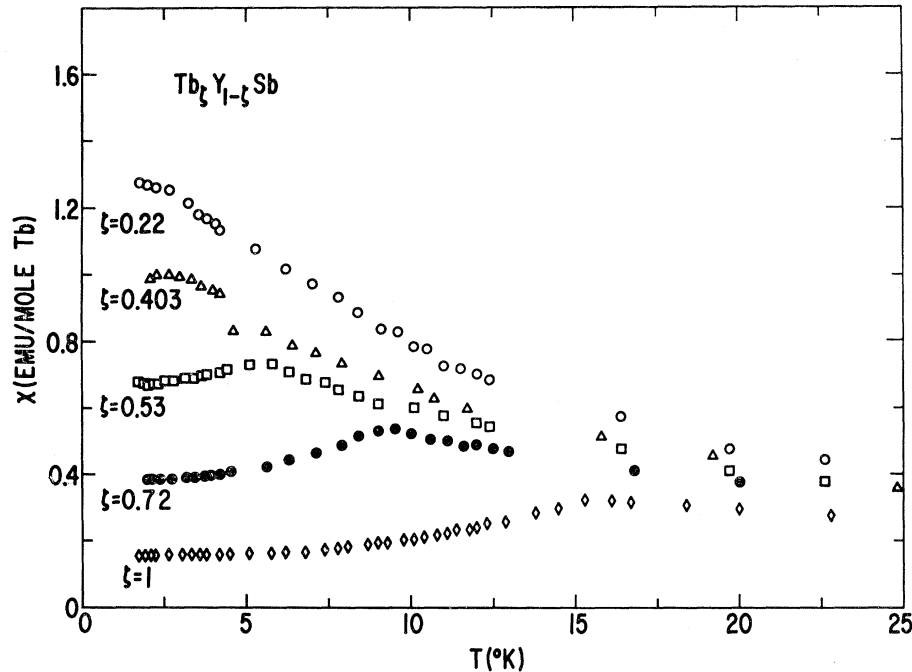


FIG. 2. Susceptibility per mole Tb as a function of temperature for $Tb_{\zeta}Y_{1-\zeta}Sb$.

creased consistently. The concentration gradient can be minimized by annealing the crystals in the above mentioned molybdenum crucibles at $1400^{\circ}C$ for about two days. The concentrations we obtained from our magnetic measurements compare fairly well with the compositions determined from the weights.

The concentrations of the samples made and their Néel temperatures are given in Table I. Nominal concentrations were obtained by choosing the proportion of Tb and Y mixed in each batch. The actual concentrations for the crystals obtained were then found by using the high-temperature (i.e., between liquid nitrogen and room temperature) susceptibility behavior to find the effective molar moment. (It is worth noting that in analyzing the magnetic behavior of the low Tb concentration crystals, the greatest uncertainty is the actual value of the Tb concentration.)

As also shown in Table I, the lattice constant has only a small variation across the entire composition range for $Tb_{\zeta}Y_{1-\zeta}Sb$.

TABLE I. $Tb_{\zeta}Y_{1-\zeta}Sb$. Summary of sample concentrations, lattice parameters, and Néel temperatures.

ζ nominal	ζ from high T moment	$a_0(\text{\AA})$	$T_N(^{\circ}K)$	ζ nominal	ζ from high T moment	$a_0(\text{\AA})$	$T_N(^{\circ}K)$
1	1	6.180	15.1	0.43	0.44	...	2.75
0.95	0.95	...	13.8	0.40	0.43	6.171	2.3
0.90	0.93	6.177	13.2	0.38	0.40 _s	...	<1.5
0.80	0.77	6.175	9.8	0.36	0.39 _s
0.70	0.72	6.174	9.2	0.30	0.31	6.170	...
0.60	0.64	6.173	8.2	0.20	0.22	6.167	...
0.50	0.53	6.171	5.0	0.10	0.10	6.167	...
0.48	0.48	...	4.0	0.05	0.05
0.46	0.47	...	3.5	0	0	6.165	...

Susceptibility measurements have been done for all the compositions shown in Table I. Magnetic susceptibilities were measured by the Faraday balance method in a conventional electromagnet with suitably shaped pole pieces. The strength of the applied field was from 3 to 13 kOe depending on the specific requirements. Low-field susceptibilities (magnetic field about 10 Oe) were measured by the mutual inductance method using a commercial ac bridge.

The results of some of the susceptibility measurements (with applied field from 3 to 13 kOe in the various cases) are shown in Fig. 2 to indicate the behavior found. The measurements were done on all samples for temperatures up to $300^{\circ}K$, but only the lower temperature results are shown. *It is important to note that in Fig. 2 the susceptibilities have been normalized to Tb concentration.*

In Fig. 2, at high Tb concentration one has the peak in susceptibility characteristic of antiferromagnetic materials. This shifts to lower temperature as the Tb concentration decreases, and at the same time the peak value of susceptibility per mole Tb shifts upward. However, in distinction to magnetic ordering in permanent moment systems, the susceptibility (normalized to Tb concentration) peak does not grow indefinitely as the Néel temperature goes to zero. Instead, at a concentration of about 40% Tb, the Néel temperature goes to zero; and for Tb concentration below that, one has a Van Vleck susceptibility which approaches the finite crystal-field-only limit at zero temperature as Tb concentration decreases further. Specific-heat experiments⁹ confirm this picture and the

⁹ W. Stutius, Physik Kondensierten Materie **9**, 341 (1969).

essentially constant behavior of the crystal field with variation of Tb concentration.

For such an induced moment system, the apparent Néel temperature, particularly when T_N is small, is sensitive to the value of applied field. Therefore, the way in which the Néel temperature goes to zero with Tb concentration has been studied by the induction technique in a field of 10 G. The results are shown in Fig. 3. The arbitrary units for each susceptibility curve shown differ, so the difference in size of peak between curves has no significance. The significant point is the shift of the peak toward lower temperature. For a terbium concentration of 40.3% there is no peak down to a temperature of 1.5°K, the lowest temperature reached. Thus the susceptibility measurements shown in Figs. 2 and 3 directly confirm the theory of a threshold value of exchange necessary to go from Van Vleck susceptibility to antiferromagnetism at very low temperatures; and this is also verified by specific-heat measurements.⁹

High-pulsed-field magnetization measurements have also been used to study the magnetic behavior with varying Tb concentration. Magnetization curves were measured in pulsed fields up to about 120 kOe. The pickup system consisted of two concentric, oppositely wound, coils with a diameter ratio of 1:2. The signal obtained by placing the sample in the null-balanced coils is integrated and displayed versus the applied field on an oscilloscope. Calibration of the magnetization was done either by comparison with the moments measured by the Faraday method or by gauging the sensitivity of the pickup coils with a Nickel sample. The crystals under investigation were x-ray oriented and sealed in plastic material of about 10 times the volume of the crystal. This encapsulation allowed heating effects to be avoided as much as possible.

Such high-field magnetization measurements have been performed for crystals with most of the concentrations shown in Table I. The results for a few concentrations are shown in Fig. 4. As Tb concentration is lowered, the behavior varies smoothly from that of pure TbSb. For concentrations equal to or below 40.3% Tb, that is equal to or below that necessary for antiferromagnetism at zero temperature, one obtains anisotropic magnetization behavior qualitatively similar in character to the crystal-field-only behavior found for TmSb. (The anisotropic magnetization behavior for four of the concentrations equal to or less than the critical concentration of 40.3% Tb are shown in Sec. 3 in connection with the discussion.)

3. ANALYSIS AND DISCUSSION

We now analyze the susceptibility, Néel temperature, and high-field anisotropic magnetization data in order to quantitatively develop our picture of the approach to the threshold for magnetic ordering in induced magnetic systems, and also to find the quantitative

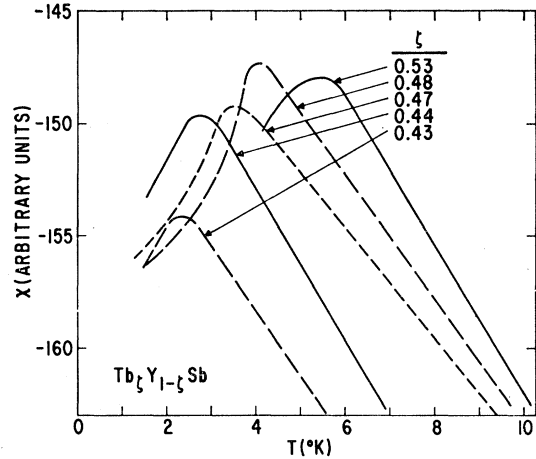


FIG. 3. Susceptibility of $Tb_{\zeta}Y_{1-\zeta}Sb$ measured by induction technique with $H=10$ Oe for values of ζ slightly greater than critical value for which $T_N=0$.

information yielded about the crystal-field and exchange effects in a system such as $Tb_{\zeta}Y_{1-\zeta}Sb$. To proceed in this aim we need a quantitative theoretical description for the approach to the ordering threshold. The theory of this threshold has been treated by several authors²⁻⁵ both in molecular field theory and in various theories including correlation effects with varying degrees of sophistication.

In this paper we shall use a molecular field theory. In doing so, besides neglecting exchange correlation effects, we shall neglect any effects associated with the inhomogeneous distribution of Tb through the samples true even for an ideal alloy (i.e., all Tb sites do not have the same arrangement of Tb neighbors). Thus we shall treat the exchange field as depending linearly on Tb concentration. The longer range the exchange, the more justified is the neglect of correlation and inhomogeneity effects. [$Tb_{\zeta}Y_{1-\zeta}Sb$ is an intermetallic compound, and the exchange mechanism is quite likely to be some variant of the Ruderman-Kittel-Kasuya-Yosida mechanism (RKKY) via polarization of the conduction electrons.]

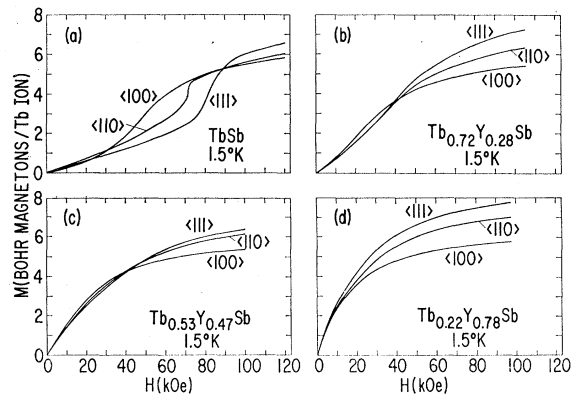


FIG. 4. Magnetization per Tb ion for $Tb_{\zeta}Y_{1-\zeta}Sb$ at 1.5°K.

A. Molecular Field Theory for Paramagnetic Susceptibility and Néel Temperature

In this subsection we treat the situation where the moment is small, that is for low field in the paramagnetic regime or at T_N in the antiferromagnetic regime. We consider the effect on an induced moment system of an exchange field linearly dependent on magnetization. (In Sec. 3 C, when discussing the nonlinear anisotropic magnetization, we will generalize to higher-order dependence on magnetization.)

In this case

$$H_{\text{eff}} = H + \lambda M \quad (3.1)$$

and

$$M = \chi_{\text{CF}} H_{\text{eff}} = \chi_{\text{CF}} (H + \lambda M). \quad (3.2)$$

Thus, dividing through by M and transposing terms gives

$$1/\chi = 1/\chi_{\text{CF}} - \lambda. \quad (3.3)$$

Then if λ scales linearly with concentration,

$$\lambda = C_{\text{ex}} \zeta, \quad (3.4a)$$

$$1/\chi = 1/\chi_{\text{CF}} - C_{\text{ex}} \zeta, \quad (3.4b)$$

where C_{ex} is constant as Tb concentration varies. Here χ_{CF} is the crystal-field-only susceptibility given by (2.6), (2.7), and (2.9) of I. As shown by (3.3), the effect of exchange in the linear molecular field approximation is to simply rigidly shift the curve of $1/\chi$ versus T downward for ferromagnetic exchange, or upward for antiferromagnetic exchange.³

For ferromagnetic ordering, the threshold value of λ (i.e., the value for which ferromagnetism first occurs at $T=0$) is that for which $1/\chi$ diverges at $T=0$. This threshold value for ferromagnetism is

$$\lambda_f = 1/\chi_{\text{CF}}(T=0). \quad (3.5)$$

For antiferromagnetism, the threshold value of λ depends on the particular type of antiferromagnetic ordering. The simplest situation corresponds to ordering where the moment of any ion is antiparallel to the moments of all neighbors with which it has exchange interaction (i.e., most simply when there is exchange with only one type of neighbor, and that exchange is antiferromagnetic). In the paramagnetic regime all moments are aligned parallel by the applied field, and for small moments^{1,3}

$$\langle M \rangle = g\mu_B \langle J_z \rangle = \chi_{\text{CF}} \left(H + \frac{2z\mathcal{J}}{g\mu_B} \langle J_z \rangle \right) \quad (3.6)$$

so that

$$\lambda = 2z\mathcal{J}/g^2\mu_B^2. \quad (3.7)$$

Here the angular brackets denote the thermal average. Equation (3.6) applies to a concentrated (i.e., homogeneous) magnetic system, where z is the number of neighbors to which each ion is coupled with exchange constant \mathcal{J} . Antiferromagnetic ordering occurs when the moments align antiparallel with infinitesimal mo-

ment in zero applied field. At the antiferromagnetic threshold:

$$g\mu_B \langle J_z \rangle = -\chi_{\text{CF}} (2z\mathcal{J} \langle J_z \rangle / g\mu_B) \quad (3.8a)$$

or

$$2z\mathcal{J}/g^2\mu_B^2 = -1/\chi_{\text{CF}}. \quad (3.8b)$$

Thus,

$$\lambda_{a1} = -1/\chi_{\text{CF}}(T=0) \quad (3.9)$$

is the critical value for λ for antiferromagnetic ordering of this type to first occur at $T=0$.

For the MnO-type antiferromagnetic ordering pertinent¹⁰ to TbSb, half of the 12 nearest neighbors of a given moment are parallel and half antiparallel to it; while the six second nearest neighbors are antiparallel.¹¹

In the paramagnetic regime all the moments are aligned parallel; and if we consider only exchange with nearest and next nearest neighbors, for small moments,

$$\langle M \rangle = g\mu_B \langle J_z \rangle = \chi_{\text{CF}} \left(\frac{H + 2[12\mathcal{J}_1 + 6\mathcal{J}_2]}{g\mu_B} \langle J_z \rangle \right) \quad (3.10)$$

so that

$$\lambda = \frac{2[12\mathcal{J}_1 + 6\mathcal{J}_2]}{g^2\mu_B^2}. \quad (3.11)$$

This is for a homogeneous system with nearest- and next-nearest-neighbor exchange constants given by \mathcal{J}_1 and \mathcal{J}_2 , respectively. Antiferromagnetic MnO-type ordering occurs when,

$$g\mu_B \langle J_z \rangle = -\chi_{\text{CF}} \left(\frac{12\mathcal{J}_2}{g\mu_B} \langle J_z \rangle \right) \quad (3.12a)$$

or

$$12\mathcal{J}_2/g^2\mu_B^2 = -1/\chi_{\text{CF}}(T=0) \quad (3.12b)$$

is the critical relationship between the exchange and crystal-field parameters for MnO-type induced antiferromagnetic ordering with infinitesimal sublattice magnetization at $T=0$. Since λ , the effective field exchange parameter in the paramagnetic regime, depends on both \mathcal{J}_1 and \mathcal{J}_2 , there is no simple relationship, such as that in (3.9), relating the value of λ when MnO-type-induced ordering at $T=0$ first occurs to χ_{CF} at $T=0$. However, as $12\mathcal{J}_1$ becomes negligible compared to $6\mathcal{J}_2$, the simple relationship of (3.9) is recovered. Using our assumption of the effective exchange coupling scaling linearly with concentration, then in a diluted system (with ζ being the concentration of magnetic species), in Eqs. (3.7), (3.8), (3.11), and (3.12) we replace the various exchange constants \mathcal{J} by $\zeta\mathcal{J}$.

The Néel temperature for MnO-type-induced ordering is determined by the generalization of (3.12b) to finite temperature.

¹⁰ H. R. Child, M. K. Wilkinson, J. W. Cable, W. C. Koehler, and E. O. Wollan, *Phys. Rev.* **131**, 922 (1963).

¹¹ For a discussion of antiferromagnetism in the molecular field model, see J. S. Smart, *Effective Field Theories of Magnetism* (W. B. Saunders Co., Philadelphia, 1966).

$$\frac{1}{\chi_{CF}(T_N)} = -\frac{12g_2\zeta}{g^2\mu_B^2}. \quad (3.13)$$

[In the limit where T_N is sufficiently high so that χ_{CF} has approximately Curie law behavior, this gives the usual expression¹¹ for T_N with MnO-type ordering. In this limit $T_N \approx -4g_2J(J+1)$.]

B. Analysis of Experimental Susceptibility ($\zeta \leq 0.403$) and Néel-Temperature ($\zeta \geq 0.403$) Behavior

Using (3.4b) we can analyze the inverse susceptibility behavior as a function of Tb concentration in the paramagnetic regime ($\zeta \leq 0.403$). For a fourth-order-only crystal field, the theoretical behavior then depends on only two parameters: W specifying the crystal field [see (2.1) and (2.3) of I] and λ , proportional to terbium concentration, giving the exchange.

We attempt to fit the experimental behavior by determining C_{ex} and W entering (3.4b) as follows. We choose C_{ex} to fit the shift in $1/\chi$ between the $\zeta=0.403$ and $\zeta=0.05$ crystals at the lowest temperatures (i.e., essentially at $T=0$). Then from (3.4b) this value of C_{ex} together with the experimental value of χ at the lowest temperature for $\zeta=0.403$ serves to determine $1/\chi_{CF}(T=0)$. From the value of $\chi_{CF}(T=0)$, by use of (2.10) of I we determine W . The values of W and λ so found are

$$\text{Tb}_\zeta\text{Y}_{1-\zeta}\text{Sb}: W = -0.396^\circ\text{K}, \quad (3.14a)$$

$$\text{Tb}_\zeta\text{Y}_{1-\zeta}\text{Sb}: \lambda = C_{ex}\zeta = -0.697 \times 10^4 \zeta \text{ Oe}/\mu_B. \quad (3.14b)$$

For this value of W , χ_{CF} as a function of temperature is determined from (2.6), (2.7), and (2.9) of I. In Fig. 5 we compare the theoretical behavior of $1/\chi$ versus T for varying Tb concentration as found from (3.4b) with the experimental results for $\zeta \leq 0.403$. (For the nominally 36% Tb sample, the scatter in the data is rather large, and we regard the composition of the crystal as questionable. For that reason, we have not included that data.) The over-all agreement of theory and experiment is quite good considering the large amount of data to be fit. The microprobe analysis indicated less uniform distribution of Tb in the 31% sample than in the others, and that may explain the scatter in data and consequent poorer agreement with the theory for that sample. Since the data are normalized per Tb ion, the experimental points at low concentration are quite sensitive to the correct determination of the Tb concentration; and therefore determination of that concentration is the largest source of possible experimental uncertainty.

[Part of the difficulty may also be to define a meaningful χ in a situation where the M -versus- H curve at low T has significant nonlinearity even below 10 kOe. This nonlinearity is discussed further below. The experimental χ given in Fig. 5 was defined as $\chi_{\text{expt}} = M/H|_{\text{low } H}$. In each case, the low H was taken as the

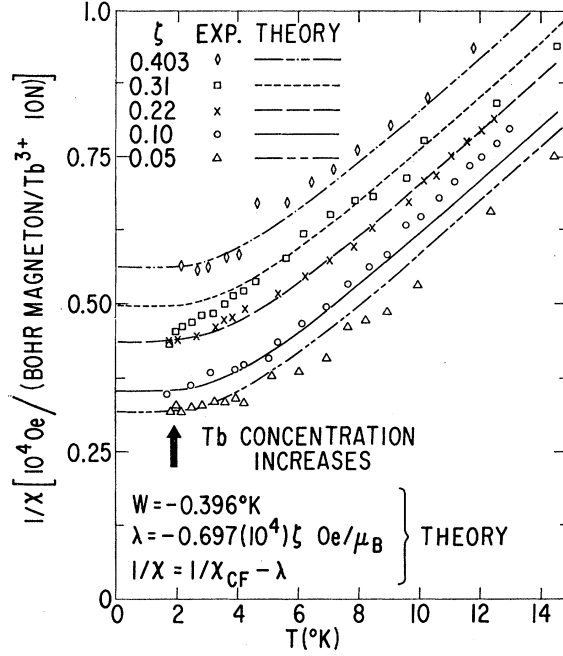


FIG. 5. Inverse susceptibility per Tb ion as a function of temperature for $\text{Tb}_\zeta\text{Y}_{1-\zeta}\text{Sb}$. Experiment is compared to molecular field theory for $\zeta \leq 0.403$.

lowest value below which there was no experimentally significant deviation of the M -versus- H behavior from linearity. For the $\zeta=0.403$, 0.22, and 0.10 crystals this low H was 5 kOe at the low- T values (1.5 to 8°K) and 13 kOe thereafter; for $\zeta=0.05$, it was 4 kOe at the low- T values shown in Fig. 5 and 13 kOe at higher T ; and for $\zeta=0.31$ and 0.396, it was 2.5 kOe at the low- T values shown in Fig. 5 and 13 kOe at higher T .]

The W found in our analysis corresponds to a Γ_1 to Γ_4 splitting of 11.9°K. This is less than half the value for TmSb.

For a critical concentration of $\zeta=0.403$, Eq. (3.9) is exactly satisfied for the values of W and C_{ex} given in (3.14). This indicates that nearest-neighbor exchange (\mathcal{J}_1) is negligible compared to second-neighbor exchange (\mathcal{J}_2). Then in theory the variation of T_K with ζ is determined by the generalization of (3.9) to finite temperature.

$$1/\chi_{CF}(T_N) = -C_{ex}\zeta. \quad (3.15)$$

[The fact that (3.9) is exactly satisfied should probably not be taken too seriously; however, even approximately satisfying (3.9) allows us to use (3.15) as a very simple approximation giving T_N . It is quite possible that the exchange is rather long range and oscillatory, so that exchange beyond the second neighbor is significant. Then satisfying (3.9) could come about through cancellation effects between some of the exchange interactions.] *We emphasize that the resulting absolute determination of T_N as ζ varies involves no further parameters other than the same W and C_{ex} giving the paramagnetic behavior.*

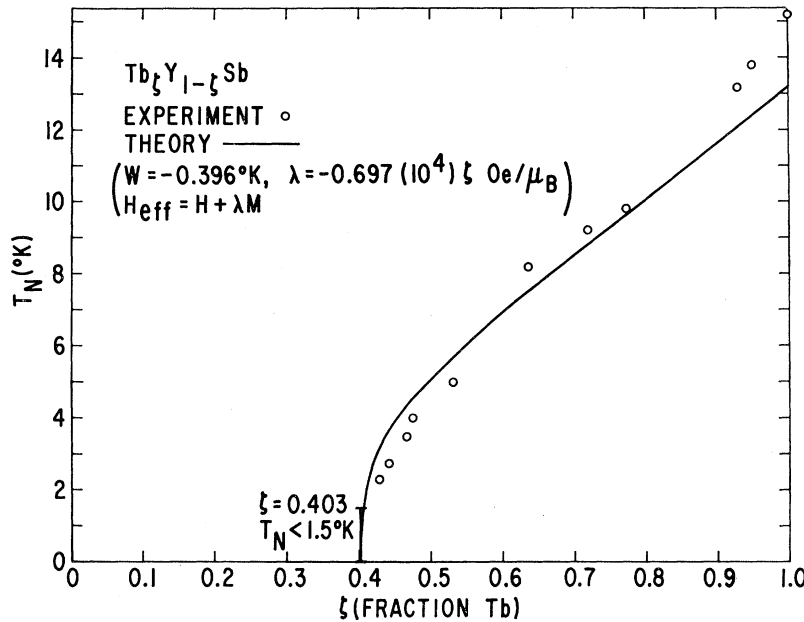


FIG. 6. Variation of Néel temperature with concentration of terbium in $Tb_{\zeta}Y_{1-\zeta}Sb$ for $\zeta \geq 0.403$.

In Fig. 6, the values of T_N obtained from (3.15) for the parameters of (3.14) are compared to experiment. [The experimental values were found by simply taking T_N as the temperature for the peak in the curve of χ versus T . In light of other uncertainties, it did not seem worthwhile to perform a more sophisticated analysis¹² to find the experimental T_N .] Once again, the agreement of experiment and the linear molecular field theory is quite good.

We should point out that a necessary consequence of a linear molecular field theory with exchange param-

eters scaled linearly with concentration is that the type of magnetic ordering at T_N is unchanged as Tb concentration varies. This should be amenable to examination by neutron diffraction.

The results of the subsection then show that one can understand the induced magnetization behavior of the $Tb_{\zeta}Y_{1-\zeta}Sb$ system for small moments on the basis of a simple linear molecular field theory where the crystal field is constant, and the exchange parameter varies linearly with Tb concentration. In particular, using only two parameters for all Tb concentrations, one has good agreement for the threshold behavior for the magnetic ordering (T_N) and for the behavior below the exchange threshold (χ) at low field where only a small magnetization is developed.

C. High-Field Nonlinear Anisotropic Magnetization ($\zeta \leq 0.403$)

Using the linear molecular field theory of (3.1) and scaling the exchange parameter with concentration as in (3.4a), it is a simple matter to find the magnetization behavior in the nonlinear regime. For the W of (3.14a) one can obtain the variation of M with H_{eff} using (2.1), (2.4), (2.5), and (2.11) of I and the calculational method described in Sec. 2 of I. Since λ is known, and since for specified M , H_{eff} is also known, H for each M is easily found from (3.1).

In Fig. 7 the experimental curves of M versus H for $Tb_{\zeta}Y_{1-\zeta}Sb$ in the regime below the ordering threshold ($\zeta \leq 0.403$) are compared to the theoretical curves found in this way. The theory uses the same parameters given in (3.14), which gave good agreement with the experimental $1/\chi$ versus T and T_N behavior as ζ varied. In each panel of Fig. 7, the curves of M versus H are shown for all three principal directions for a concen-

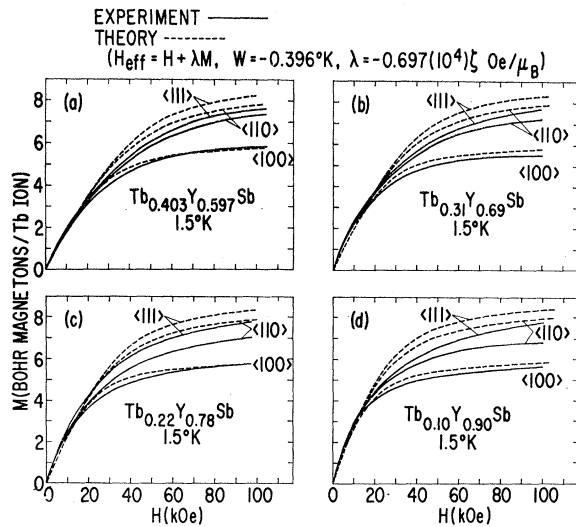


FIG. 7. Magnetization per Tb ion for $Tb_{\zeta}Y_{1-\zeta}Sb$ at $1.5^{\circ}K$ for $\zeta \leq 0.403$. Experiment is compared to linear molecular field theory. Each panel shows anisotropic magnetization for the indicated concentration.

¹² H. Callen, W. P. Wolf, and J. S. Kouvel, J. Appl. Phys. 37, 1172 (1966).

tration less than or equal to the critical concentration of Tb for antiferromagnetism. This is a useful mode of presentation for seeing the development of the anisotropic magnetization. As shown in Fig. 8, it is also useful to show the variation with concentration for each principal direction. In Fig. 8, the crossing of the experimental curves at high fields for the differing concentrations, which occurs for the $\langle 110 \rangle$ and $\langle 100 \rangle$ directions, probably reflects the uncertainty in measurement in that regime of magnetic field.

We see that the behavior at high fields in the nonlinear regime is not explained by the linear molecular-field theory using the values of crystal field and exchange parameters that describe the susceptibility and Néel temperature behavior. (Our criterion for "good agreement" between theory and experiment is that obtained^{6,7} for TmSb at 1.5°K.) In particular, there is an indication that the nonlinearity and anisotropy of the magnetization develops at somewhat lower fields than expected from the linear molecular field theory.

We note that one might be tempted to improve the agreement between theory and experiment by introducing some sixth-order crystal-field anisotropy, letting x vary from -1 toward 0. However, to lower the theoretical $\langle 111 \rangle$ high-field magnetization by varying x would involve going quite close to $x=0$, almost completely sixth-order anisotropy. From our studies^{6,7,13} of TmSb and TmN, this appears unlikely. Also, if one went to $x=0$, the $\langle 100 \rangle$ magnetization would increase markedly, giving poor agreement with theory. (See Fig. 4 of I.) In fact for $x=0$, there is very little anisotropy in the magnetization, and the hard directions are $\langle 110 \rangle$.

The behavior shown in Figs. 7 and 8 suggests the importance of higher order (in the magnetization) exchange effects than those leading to a linear molecular field. To see the sort of effects found on the theoretical behavior by adding higher-order exchange, in Fig. 9 we include a term in the effective field with cubic dependence on the magnetization such as would arise from a biquadratic exchange. [The crystal-field parameters are the same as in Figs. 5–8, and the exchange parameters have been chosen so that the low-field behavior is well matched. Then the kind of agreement found in Figs. 5 and 6 (with χ defined as M/H at low field) would continue to hold.]

The third-order exchange field parameters $D_{\langle 111 \rangle}$, $D_{\langle 110 \rangle}$, and $D_{\langle 100 \rangle}$ have been taken to scale with concentration, and have been chosen as described below to satisfy cubic symmetry.

For a cubic material, the fourth-order contribution to the free energy from exchange takes the form

$$F_4 = aM^4 + b(M_x^4 + M_y^4 + M_z^4). \quad (3.16)$$

Then the corresponding effective field giving an in-

¹³ B. R. Cooper, R. C. Fedder, and D. P. Schumacher, Phys. Rev. Letters 18, 744 (1967); Phys. Rev. 168, 654 (1968).

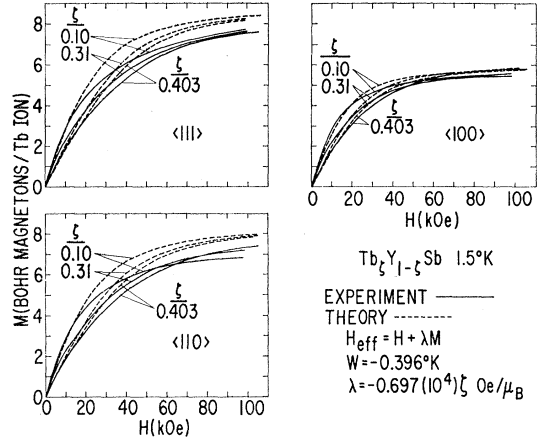


FIG. 8. Magnetization per Tb ion for $Tb_{\zeta}Y_{1-\zeta}Sb$ at 1.5°K for $\zeta \leq 0.403$. Experiment is compared to linear molecular field theory. Each panel shows magnetization curves for several concentrations in indicated principal direction.

duced magnetization is

$$H_{4\text{eff}} = DM^3 = -\frac{\partial F_4}{\partial M} = -4M^3[a + b(\sin^4\theta \cos^4\varphi + \sin^4\theta \sin^4\varphi + \cos^4\theta)], \quad (3.17)$$

where θ and φ are the usual polar and azimuthal angles in spherical coordinates with a crystal axis as the polar axis. [We note that the effective field defined in (3.17) is not the same as that entering into the collective-mode behavior in a permanent moment system, as in ferromagnetic resonance, for small angular variation about equilibrium of the magnetization.] This gives

$$D_{\langle 100 \rangle} = -4(a+b), \quad (3.18a)$$

$$D_{\langle 110 \rangle} = -4(a + \frac{1}{2}b), \quad (3.18b)$$

$$D_{\langle 111 \rangle} = -4(a + \frac{1}{3}b), \quad (3.18c)$$

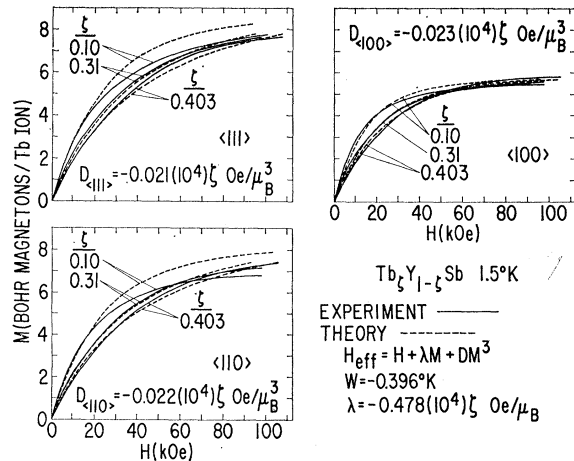


FIG. 9. Magnetization per Tb ion for $Tb_{\zeta}Y_{1-\zeta}Sb$ at 1.5°K for $\zeta \leq 0.403$. Experiment is compared to theory including cubic molecular field. Each panel shows magnetization curves for several concentrations in indicated principal direction.

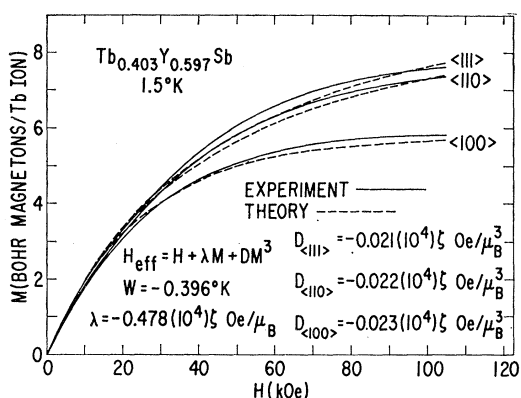


FIG. 10. Magnetization per Tb ion of $Tb_{0.403}Y_{0.597}Sb$ at $1.5^\circ K$ compared to theory including cubic molecular field.

so that for cubic symmetry

$$D_{\langle 100 \rangle} = 4D_{\langle 110 \rangle} - 3D_{\langle 111 \rangle}. \quad (3.19)$$

The theoretical curves in Fig. 9 were then obtained using the same value of the crystal-field parameter, $W = -0.396^\circ K$, used earlier, and taking

$$H_{\text{eff}} = H + \lambda M + DM^3, \quad (3.20)$$

where D is allowed to differ for the three principal directions subject to the condition (3.19).

Once λ and D are specified, the M -versus- H curve is obtained from (3.20) in a way quite similar to that used above for a linear molecular field. Since W is specified, the curve of M versus H_{eff} is known, so that for each M , (3.20) can be used to find the corresponding H .

The values of λ and D used in the calculation were chosen as follows. The parameters λ and $D_{\langle 111 \rangle}$ were chosen by fitting the $\langle 111 \rangle$ magnetization for $\zeta = 0.403$ at one low-field and one high-field magnetization. The $D_{\langle 110 \rangle}$ was chosen by using the same λ and fitting the $\zeta = 0.403$ $\langle 110 \rangle$ magnetization at one high-field value. Finally, $D_{\langle 100 \rangle}$ was chosen to satisfy (3.19). The values so obtained are:

$$\lambda = C_{\text{ex}}\zeta = -0.478\zeta \text{ Oe}/\mu_B, \quad (3.21a)$$

$$D_{\langle 111 \rangle} = -0.0212 \times 10^4 \zeta \text{ Oe}/\mu_B^3, \\ D_{\langle 110 \rangle} = -0.0217 \times 10^4 \zeta \text{ Oe}/\mu_B^3, \quad (3.21b)$$

$$D_{\langle 100 \rangle} = -0.0232 \times 10^4 \zeta \text{ Oe}/\mu_B^3.$$

The D 's so obtained in (3.21b) are almost isotropic. However, this result should not be taken too seriously as an indication of isotropy in the higher-order exchange effects. Indeed, the agreement between theory and experiment in Fig. 9, while better than that of the linear theory of Figs. 7 and 8, still needs improving. In

particular, as shown in Fig. 10, the experimental magnetization indicates the development of anisotropy at lower fields than the theory. (This early development of the anisotropy is borne out by very accurate dc magnetization measurements currently in progress.¹⁴)

The difficulty of finding agreement between the experimental high-field anisotropic magnetization and the theory including a linear, or even a cubic, molecular field is not too surprising. The real description of the behavior in high fields is probably more complex than can be described by one, or a few, field- and magnetization-independent exchange parameters. Indeed, this can be expected to be the case in systems such as this where there are large orbital contributions to the magnetic moment. The form of the effective exchange interaction in such systems depends on the detailed shape of the $4f$ wave functions, and can have substantial anisotropic higher-order contributions.¹⁵ In the present experiments one knows that in the crystal-field-only limit one changes the nature of the $4f$ wave functions drastically on going to the highest fields. Thus one can expect correspondingly large changes in the effective exchange.

The point to be stressed, however, is that one is changing the crystal-field wave functions in a controlled, well-understood way by applying high magnetic fields. Thus one can hope to explain the changes in effective exchange as a function of applied field on a first-principles basis. This means that anisotropic magnetization experiments of the present type may be valuable in providing basic information on the orbital effects on effective exchange interaction. In this regard, very accurate dc magnetization experiments on the $Tb_{\zeta}Y_{1-\zeta}Sb$ system in fields up to approximately 100 kOe, are currently in progress by Jacobs in cooperation with the present authors. These experiments should be particularly useful in identifying higher-order exchange effects such as the development of significant anisotropy in the magnetization at relatively low fields.

ACKNOWLEDGMENTS

We are most grateful to Professor G. Busch for his stimulating interest, and to Dr. I. S. Jacobs and Professor W. P. Wolf for much interesting and useful discussion. We wish to thank Miss E. Kreiger for her aid with the numerical calculations, and Miss I. Schneider for her aid in preparing the crystals and performing the measurements.

¹⁴ I. S. Jacobs (private communication).

¹⁵ K. W. H. Stevens, *Rev. Mod. Phys.* **25**, 166 (1953); J. H. Van Vleck, *Rev. Mat. Fis. Teor. (Tucuman, Argentina)* **14**, 189 (1962); P. M. Levy, *Phys. Rev. Letters* **20**, 1366 (1968); *Phys. Rev.* **177**, 509 (1969); R. J. Elliott and M. F. Thrope, *J. Appl. Phys.* **39**, 802 (1968); R. J. Birgenau, M. T. Hutchings, J. M. Baker, and J. D. Riley, *ibid.* **40**, 1070 (1969).